Since January 2020 Elsevier has created a COVID-19 resource centre with free information in English and Mandarin on the novel coronavirus COVID-19. The COVID-19 resource centre is hosted on Elsevier Connect, the company's public news and information website.

Virology 551 (2020) 84–92

Contents lists available at ScienceDirect

Virology

journal homepage: www.elsevier.com/locate/virology

Bat mammalian orthoreoviruses cause severe pneumonia in mice

Ren-Di Jiang[a,b], Bei Li[a], Xiang-Ling Liu[a], Mei-Qin Liu[a,b], Jing Chen[a,b], Dong-Sheng Luo[a,b], Bing-Jie Hu[a,b], Wei Zhang[a], Shi-Yue Li[c], Xing-Lou Yang[a,**], Zheng-Li Shi[a,*]

[a] CAS Key Laboratory of Special Pathogens and Biosafety, Wuhan Institute of Virology, Chinese Academy of Sciences, Wuhan, China
[b] University of Chinese Academy of Sciences, Beijing, China
[c] Wuhan University, Wuhan, China

ARTICLE INFO

Keywords:
Bat
Mammalian orthoreovirus
Pathogenicity
Pneumonia

ABSTRACT

Mammalian orthoreovirus (MRV) infections are ubiquitous in mammals. Increasing evidence suggests that some MRVs can cause severe respiratory disease and encephalitis in humans and other animals. Previously, we isolated six bat MRV strains. However, the pathogenicity of these bat viruses remains unclear. In this study, we investigated the host range and pathogenicity of 3 bat MRV strains (WIV2, 3 and 7) which represent three serotypes. Our results showed that all of them can infect cell lines from different mammalian species and displayed different replication efficiency. The BALB/c mice infected by bat MRVs showed clinical symptoms with systematic infection especially in lung and intestines. Obvious tissue damage were found in all infected lungs. One of the strains, WIV7, showed higher replication efficiency in *vitro* and *vivo* and more severe pathogenesis in mice. Our results provide new evidence showing potential pathogenicity of bat MRVs in animals and probable risk in humans.

1. Introduction

Mammalian orthoreoviruses (MRVs) belong to the genus *Orthoreorivus* in the *Reoviridae* family with ten segmented double-stranded RNA genomes (Day, 2009; Mayor et al., 1965). MRVs are the prototype of reovirus, and four serotypes have been defined according to the anti-MRV serum neutralising reaction and the capacity to inhibit hemagglutination (Attoui et al., 2001; Rosen, 1960; Sabin, 1959; Vasquez and Tournier, 1962). They are widely distributed around the world. Infectious viral particles can be found in river water and raw sewage (Matsuura et al., 1988, 1993). Since its discovery, human MRVs have been isolated repeatedly from respiratory and enteric tract samples of children. Although they usually cause mild respiratory/gastrointestinal symptoms or asymptomatic illness (El-Rai and Evans, 1963; Leers and Rozee, 1966; Sabin, 1959), some cases have recently been reported in humans, showing that MRVs were responsible for severe pneumonia and encephalitis (Ouattara et al., 2011; Steyer et al., 2013; Tyler et al., 2004).

Bats are the only flying mammals with more than 50 million years of evolutionary history (Teeling et al., 2005). Bats are well known as natural reservoirs of some important human pathogens, such as severe acute respiratory syndrome-related coronavirus (SARS-CoV), Marburg virus and Nipah virus (Botvinkin et al., 2003; Chua et al., 2002; Ge et al., 2013; Leroy et al., 2005; Yang et al., 2015a). Orthoreoviruses have been detected in bats worldwide (Jansen van Vuren et al., 2016; Lelli et al., 2015; Lorusso et al., 2015; Yang et al., 2015b). The known bat orthoreoviruses are mainly divided into 2 groups, Pteropine orthoreoviruses (PRVs) and bat MRVs (Kohl et al., 2012; Lelli et al., 2013; Li et al., 2016). Some PRVs, such as Melaka virus and Kampar virus, isolated from bats have been suspected to be responsible for human diseases (Chua et al., 2007, 2008). There have been some studies on the pathology of bat PRVs and MRVs isolated from other mammals (Egawa et al., 2017; Kanai et al., 2018; Li et al., 2015). However, the pathogenicity of bat MRVs in humans and animals remains unclear.

Previously, we isolated 6 MRV strains from bat faeces and urine samples (Yang et al., 2015b), and their genomic sequences have high similarity with the isolates from ill mink, piglets or children (Dai et al., 2012; Lian et al., 2013; Ouattara et al., 2011). These bat MRVs belong to mammalian orthoreovirus serotype 1, 2 or 3. However, their pathogenicity and interspecies transmission potentials have not been analysed. In this study, we selected each of the 3 serotypes and assessed their host range in different cell lines and pathogenesis in mice.

* Corresponding author. Wuhan Institute of Virology, Chinese Academy of Sciences, 44 Xiao Hong Shan, 430071, Wuhan, Hubei, China.
** Corresponding author. Wuhan Institute of Virology, Chinese Academy of Sciences, 44 Xiao Hong Shan, 430071, Wuhan, Hubei, China.
E-mail addresses: yangxl@wh.iov.cn (X.-L. Yang), zlshi@wh.iov.cn (Z.-L. Shi).

https://doi.org/10.1016/j.virol.2020.05.014
Received 4 November 2019; Received in revised form 3 March 2020; Accepted 27 May 2020
Available online 22 June 2020

2. Materials and methods

2.1. Ethics statement

All of the animals infected with bat MRVs were handled in biosafety level 2 animal facilities in accordance with the recommendations for care and use of the Institutional Review Board of Wuhan Institute of Virology of the Chinese Academy of Sciences (ethics number WIVA05201401). The mice were inoculated with virus under proper anaesthesia, and all efforts were made to minimise any potential pain and distress.

2.2. Viruses and cell lines

Bat MRV-WIV2, WIV3 and WIV7, representing serotype 1, 2 and 3, respectively, were isolated from bat samples as previously described (Yang et al., 2015b). All viruses were propagated and titrated in African green monkey kidney cells (Vero E6) (ATCC CRL-1586). The virus supernatant was serially diluted in Dulbecco's modified Eagle's medium (DMEM) (Gibco, Waltham, USA) and added to Vero E6 cells seeded in a 96-well plate. After 1 h of incubation, the supernatant was removed, and DMEM supplemented with 2% with foetal bovine serum (FBS) (Gibco, Waltham, USA) were added. Plates were observed daily for 5–7 days to track development of cytopathic effect (CPE). Median tissue culture infectious dose ($TCID_{50}$) were calculated by the Reed-Muench formula.

Myotis ricketti kidney (MdKi), *Hipposideros pratti* lung cells (HpLuT) and *Pteropus alecto* kidney cells (PaKi) were grown in Dulbecco's Modified Eagle Medium/Nutrient Mixture F-12 (DMEM/F-12) (Gibco, Waltham, USA) supplemented with 10% FBS at 37 ˚C and 5% CO_2. Human alveolar basal epithelial cells A549 (ATCC CCL-185), human cervix cells Hela (ATCC CCL-2), monkey kidney cells LLC-MK2 (ATCC CCL-7), feline kidney cells FK (ATCC CCL-94) and Madin-Darby canine kidney cells MDCK (ATCC CCL-34) were grown in DMEM supplemented with 10% FBS at 37 ˚C and 5% CO_2.

2.3. Cell tropism test

Cells were seeded in 24 well-plates 1 day before and infected with virus at multiplicity of infection (MOI = 1) (Ge et al., 2013). After 24 h of infection, cells were washed with phosphate-buffered saline (PBS), fixed with 4% paraformaldehyde and permeabilised with 0.1% Triton X-100. The permeabilised cells were blocked with bovine serum albumin (BSA) (Sangon Biotech, Shanghai, China) and then incubated with primary antibodies (rabbit anti-WIV3 polyclonal antibody). The cells were washed with PBS and stained with the fluorescein isothiocyanate (FITC)-labelled mouse anti-rabbit secondary antibody (PTGLab, Rosemont, USA) and 4′,6-diamidino-2-phenylindole, dihydrochloride (DAPI) (Roche, Basel, Switzerland). Images were acquired using an FV1200 confocal microscope (Olympus, Tokyo, Japan). Growth curve was determined by reverse transcription polymerase chain reaction (RT-qPCR) described below. Briefly, 200 μL of cell culture supernatant was collected at 0, 12, 24, 48 and 72 h post-infection (hpi) from seeded cells, respectively. Viral RNA was extracted, and RT-qPCR was performed to determine the viral load.

2.4. Animal infection experiments

Four-week-old female BALB/c mice (Laboratory Animal Centre of Wuhan Institute of Virology, CAS) were anaesthetized with 250 mg/kg of Averdin (Sigma-Aldrich, St. Louis, USA) before animals were inoculated intranasally with 10^5 $TCID_{50}$ of WIV2, WIV3, WIV7 or the DMEM as mock control. Clinical symptoms and body weight were monitored every day up to 21 days. Virus replication and pathogenesis were determined on tissues collected from mice at 1, 3, 5, 7, 10, 14 and 21 days post-infection (dpi). Serum samples were separated from the whole blood by clotting at 37 ˚C for 1 h and centrifugation at 3,000 × g for 10 min.

2.5. Histopathology and immunohistochemistry (IHC)

The collected tissues were sectioned and used for haematoxylin and eosin (H&E) staining and IHC for the detection of MRV antigen. For IHC, paraffin-dehydrated tissue sections were placed in antigen repair buffer for antigen retrieval in a microwave oven. Slices were placed in 3% hydrogen peroxide solution and incubated with light to block endogenous peroxidase. The tissue was uniformly covered with 3% BSA and incubated at room temperature. A primary antibody (rabbit anti-WIV 3 polyclonal antibody) was added dropwise to the sections and then washed in PBS. After the slices were slightly dried, tissues were covered with horseradish peroxidase (HRP) labelled against rabbit immunoglobulin G (IgG, Proteintech, Rosemont, USA). After washing in PBS, freshly prepared 3,3′-diaminobenzidine (DAB) solution was added, and then the nuclei were incubated with haematoxylin. The image information was collected using the Pannoramic MIDI system (3DHISTECH, Budapest, Hungary).

2.6. Virus replication determination in vivo

All tissues (heart, liver, spleen, lung, kidney, intestine and brain) were collected from mice infected with WIV2, WIV3 or WIV7 after euthanasia, then weighed and homogenised in 1 mL of D-Hanks buffer solution with Tissue Lyser II (Qiagen, Dusseldorf, Germany). After centrifugation, 200 μL of supernatant was used to extract viral RNA by QIAamp 96 Virus o HT Kit with Qiaxtractor system (Qiagen, Dusseldorf, Germany) according to the manufacturer's instructions. The viral RNA copy numbers were determined with RT-qPCR as follows. The forward and reverse primers were specifically designed according to bat MRV WIV 2, WIV 3 and WIV 7 RdRp sequence (forward: 5′- AGCCAAGCKAGAATAGCAAC-3′, reverse: 5′- TGCGATARATCTGGAATCTCATC-3′). The RNA template was incubated at 90 ˚C for 4 min and then 4 ˚C for 5 min before use. RT-PCR was performed by a C1000 THERMAL CYCLER 96W SYS (Bio-Rad, Hercules, USA) with a PrimeScript™ RT Master Mix (Perfect Real Time) (TaKaRa Bio, Kusatsu, Japan). The reverse transcription experimental protocol was as follows: reverse transcription (37 ˚C for 15 min), denaturation (85 ˚C for 5 s) and stored at 4 ˚C. Then, cDNA was quantified using a StepOne system (ABI, Waltham, USA) with SYBR Premix Ex Taq II kit (TaKaRa Bio, Kusatsu, Japan). The PCR protocol was 10 min at 95 ˚C and 40 cycles of 95 ˚C for 15 s and 60 ˚C for 30 s. In this study, the standard controls for MRV were the constructed plasmid containing part of the L1 segments of bat MRV WIV 3. The viral RNA copy numbers were plotted using the StepOne software programme (ABI, Waltham, USA).

2.7. Cytokine-related gene expression

Homogenised lungs were prepared as described previously. One hundred microliters of suspension were used to extract host mRNA with RNAprep Pure Cell/Bacteria Kit (TIANGEN, Beijing, China). Relative RT-qPCR was performed as described previously (Zeng et al., 2016). The primer sequences were used for amplification of target genes (Supplementary Table S1). The 18s rRNA was used as the endogenous control to normalise the input of cDNA. The cytokine-related gene expression was determined using StepOne software.

2.8. Statistical analyses

Statistical analyses were performed using PRISM™ 5.01 for Windows (GraphPad, San Diego, USA). Significant differences between groups were determined using two-way analysis of variance (ANOVA).

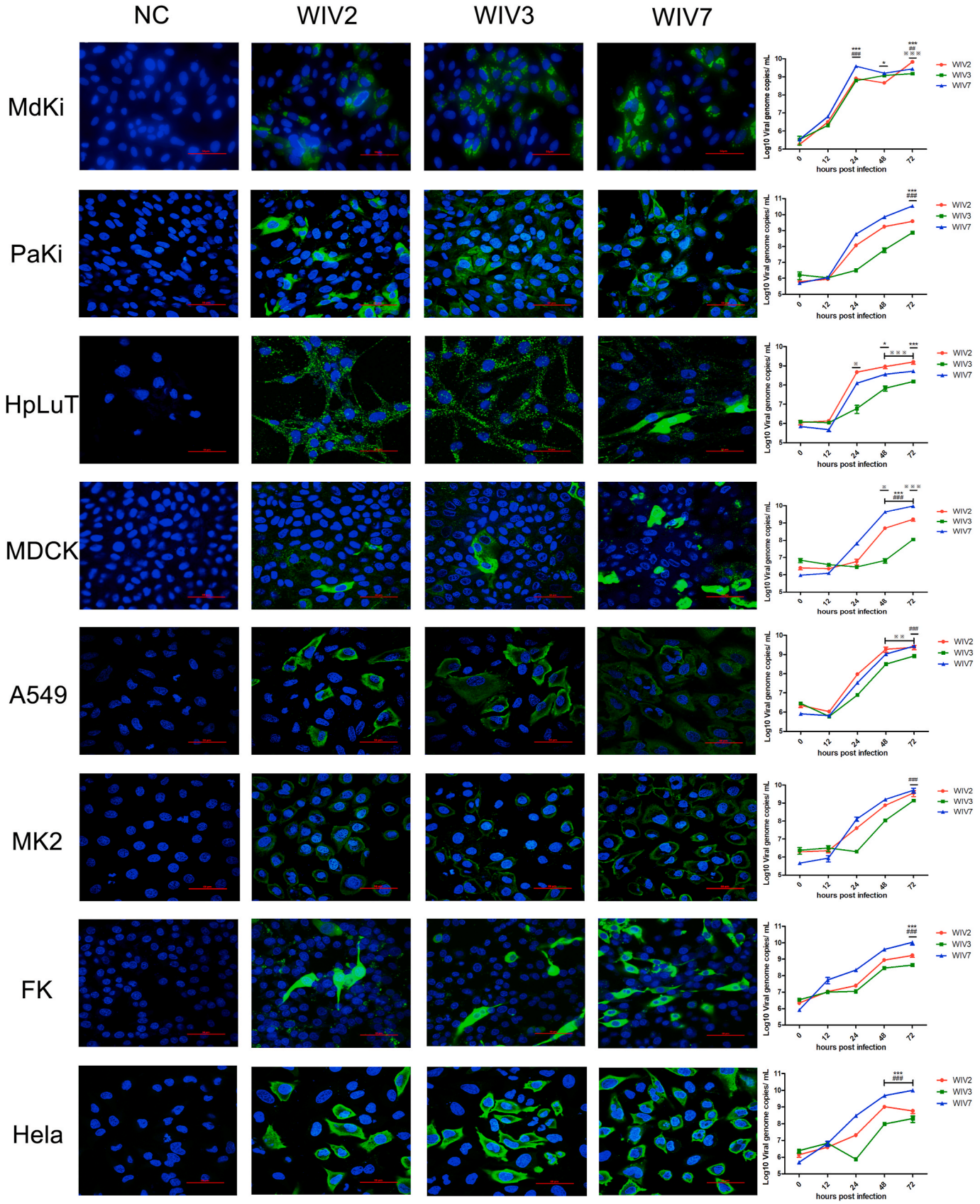

Fig. 1. Bat MRVs have wide cell tropism. MdKi, PaKi, HpLuT, MDCK, A549, LLC-MK2, FK and Hela cells were infected with bat MRV WIV2, WIV3 and WIV7 (MOI = 1). Immunofluorescence assay (Panel 1–4) was performed at 24 hpi. Bat MRV antigens were stained with rabbit anti-WIV3 polyclonal antibody as the primary antibody followed by FITC-labelled mouse anti-rabbit IgG and coloured in green. Cell nuclei were stained with DAPI and shown in blue. Scale bar is 50 μm. Multi-cycle supernatants were taken at 0, 12, 24, 48 and 72 hpi. Viral loads were determined by RT-qPCR (panel 5). Error bar indicates the standard error. * represent WIV-2 group compared with WIV-7 group, # represent WIV-3 group compared with WIV-7 group, ※ represent WIV-2 group compared with WIV-3 group. *$P < 0.05$, **$P < 0.01$, ***$P < 0.001$.

3. Result

3.1. Bat MRVs showed broad cell tropism in vitro

All cell lines, including from human, monkey, dog, cat and bat, were susceptible to the 3 bat MRVs. Growth kinetics showed that the 3 viruses have different replication efficiency (Fig. 1). WIV7 showed highest replication efficiency in 6 out of 8 tested cell lines. WIV2 replicated better than WIV3 in all tested cell lines.

3.2. Bat MRVs caused diseases in mice

To investigate the pathogenicity of the bat MRVs, 4-week-old female BALB/c mice were inoculated with 10^5 $TCID_{50}$ of bat MRV WIV2, WIV3 and WIV7, respectively, via the intranasal route. Mice in all infected groups showed clinical symptoms, such as body weight loss, piloerection and shrink. WIV2-infected mice showed body weight loss on day 1 and 2, immediately recovered on day 5 and dropped again until day 7. WIV3-infected mice showed decreased body weight loss from day 5 and recovered on day 7. WIV7-infected mice developed severe body weight loss from day 3 and recovered on day 10 but with a lower body weight than WIV2- and 3-infected animals at the end of experiments (Fig. 2). WIV7, not WIV2 and 3, showed decreased body temperature (data not shown) since 1 dpi. No mortality was observed at the end of experiments for all infected animals.

3.3. Viral replication in mice

To further characterise bat MRV replication in mice, viral RNA copies in different organs were determined by RT-qPCR (Fig. 3, Supplementary Fig. S2). All these strains cause systemic infection in mice. Viruses replicated well in the lungs, spleen, liver and intestines. The highest viral load was observed in the lungs for all strains followed by the intestines. WIV2 replicated better than WIV3 in all tested cell lines, but it wasn't detected in brain in contrast to WIV3 was detected from on day 10 till the end point. WIV7 showed higher replication efficiency in mice than the other 2 strains by exhibiting a higher viral load and longer persistence of infection in most tested organs, especially the brain. A low level of viremia was found only in WIV7-infected mice serum between 3 and 7 dpi (Supplementary Table S2).

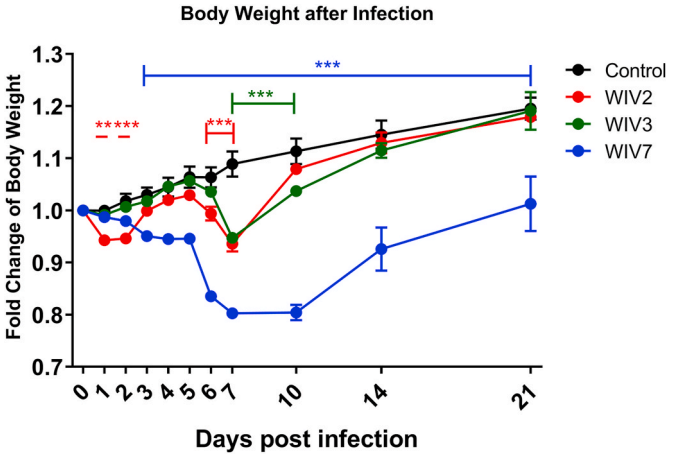

Fig. 2. Body weight changes after viral infection. Four-week-old female BALB/c mice were infected with 10^5 $TCID_{50}$ bat MRV WIV2, WIV3 or WIV7 via the internasal route. Body weights were measured at 0, 1, 2, 3, 4, 5, 6, 7, 10, 14 and 21 days post-infection. Error bar indicates the standard error. $^{**}P < 0.01$, $^{***}P < 0.001$, compared with control group.

3.4. Tissue damage in virus-infected mice

Pathological examinations were performed on all tissues of infected mice at 7 and 14 dpi with a mock-infected mouse tissue as the control (Fig. 4A and E, Supplemenaty Fig. S1). Obvious tissue damage and inflammation were found in all infected lung sections. WIV2- and WIV3-infected lungs showed distinct alveolar thickness and with some lymphocytic infiltration around vessels (Fig. 4 B, C Supplementary Fig. S1). In WIV7-infected mice, alveoli structure decreased massively in lungs and exhibited more lymphocytic infiltration in interstitial tissue (Fig. 4 D). No differences were observed in other tissues compared with the control group for all tested viruses (Supplementary Fig. S3). Viral antigens were detected in lung lesion areas by IHC staining (Fig. 4 F, G and H).

3.5. Immune response in virus-infected mice

To determine the immune response in bat MRV-infected mice, mouse serum and lungs were used to test the virus-neutralising antibody and transcriptional levels of inflammatory cytokines and chemokines. Our results showed that all virus-infected mice produced specific neutralising antibodies (Fig. 5A). WIV7 infection induced faster and higher antibody response than WIV2 and WIV3. Innate immune response was significantly increased during infection by all strains. The transcriptional level of interferon-β (IFN-β) and interferon-γ (IFN-γ) in lungs raised rapidly in the early infection of WIV2 and was maintained to the end time point. For WIV3, the mRNA level of those genes increased at 7 dpi, peaked at 14 dpi and decreased at 21 dpi. WIV7 induced a low level of gene transcriptions compared with WIV2 and WIV3 (Fig. 5B). All infected mice showed a significant increase in transcription levels of inflammatory cytokines and chemokines, including interleukin-1β (IL-1β), macrophage inflammatory protein 1-alpha (MIP1-α), interferon gamma-induced protein 10IP-10, tumour necrosis factor (TNF), RANTES (regulated upon activation normal T cell expressed and secreted) and monocyte chemoattractant protein-1 (MCP-1), compared to the control group. WIV2 induced higher and rapid inflammation reaction at the beginning of infection than the other 2 strains. The inflammation reaction induced by WIV3 and WIV7 increased gradually and peaked in the mid-period and late phase of infection, respectively (Fig. 5C).

4. Discussion

Reovirus is an enteric respiratory virus that is easily transmitted via the oral-faecal route. Previous studies have demonstrated that bat MRVs are ubiquitous, and some of them may cause clinical diseases (Chua et al., 2007, 2008; Du et al., 2010; Hu et al., 2014; Pritchard et al., 2006; Voon et al., 2011; Waruhiu et al., 2017; Yang et al., 2015b). Bat MRV WIV2, 3 and 7 belong to MRV serotype groups 1–3, respectively, and were isolated from 2 different bat species (*Myotis* and *Hipposideros* bats). Specifically, bat MRV WIV3 and 7 have a high nucleotide identity to a human isolate MRV-Tou05 and a piglet strain, respectively, based on the S1 fragment. These similarities drive us to question whether these bat MRVs have the potential to infect other animals and humans. With this in mind, we investigated the potential pathogenesis of the 3 selected bat MRVs by *in vivo* and *in vitro* infections. Our results demonstrated that the 3 bat MRVs have a wide cell tropism *in vitro* and *in vivo*. The infected mice all display obvious clinical illness, such as body weight loss and lung damage, but without any mortality. All the strains caused a systematic and persistent infection in animals at the end of the experiment of 21 dpi.

The 3 bat MRVs showed different profiles of tissue tropism and replication efficiency. All the viruses replicated in heart, liver, spleen, lung, intestine and brain tissues, with the highest replication in the lungs followed by the intestines. Among the three strains, WIV7 showed highest replication efficiency in 6 out of 8 tested cell lines. *In vivo*, higher replication of WIV7 were also detected in lungs even up to 10 dpi compared with WIV2 and WIV3, as well as in brain, which may

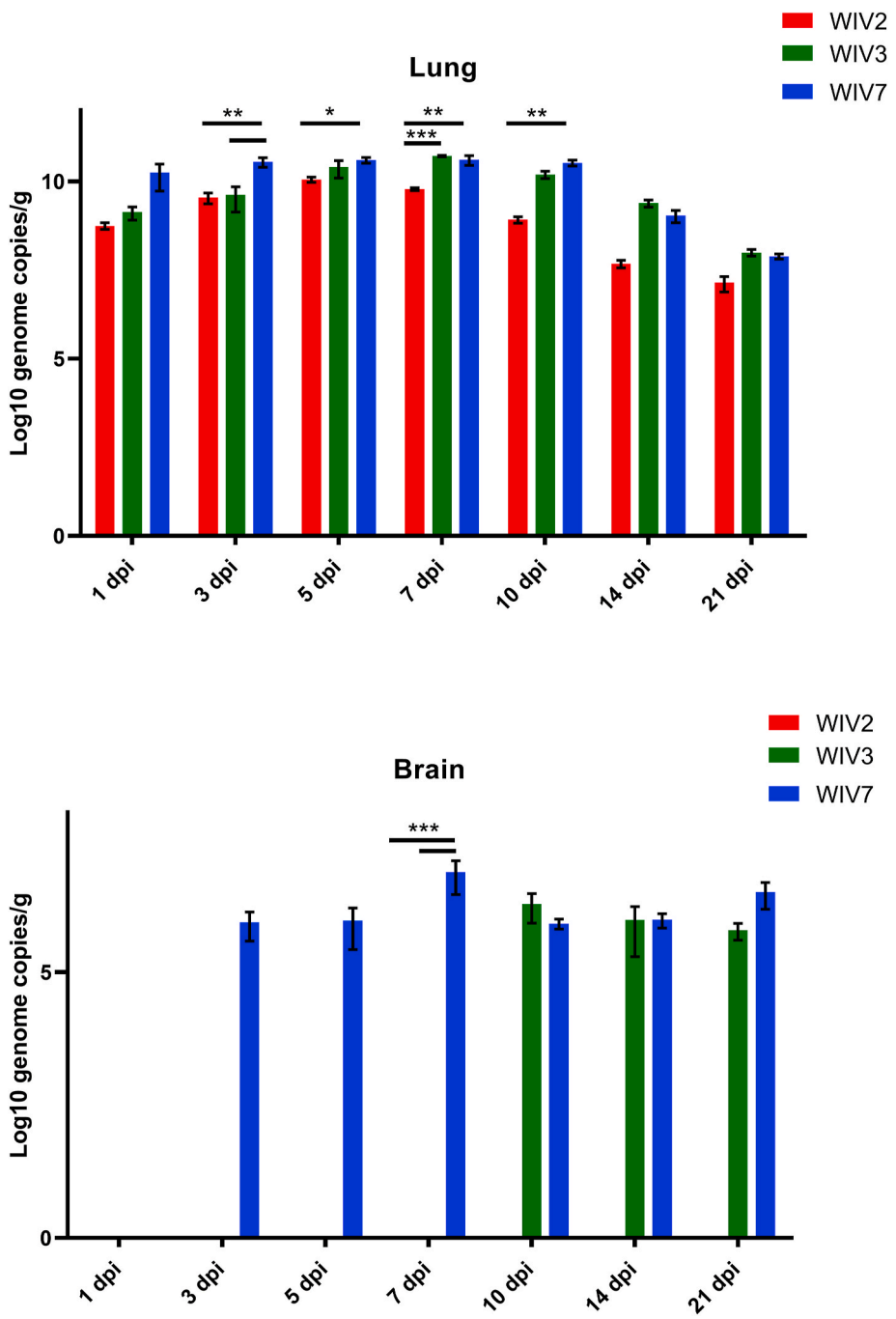

Fig. 3. Viral RNA load in lung and brain tissues after bat MRV infection. Lung and brain from infected BALB/c mice at 1, 3, 5, 7, 10, 14 and 21 dpi were detected for viral RNA load. WIV2, WIV3 and WIV7 show different infection efficiency in BALB/c mice. N = 3 in each time point. Error bar indicates the standard error. Black underline represent the comparison between indicated groups, $^{*}P < 0.05$, $^{**}P < 0.01$, $^{***}P < 0.001$.

facilitate its high pathogenicity. In addition, low level of viremia was observed only in WIV7 infected mice at early stage of infection, which may help the virus dissemination for systemic infection. WIV7-infected mice, alveoli structure decreased massively in lungs and exhibited more lymphocytic infiltration than WIV2- and WIV3-infected lung tissues which also showed distinct alveolar thickness and with some lymphocytic infiltration around vessels.

All viruses induce innate and adaptive immune response in mice but at different infection stage. Interferon and inflammatory cytokines/chemokines transcriptional production increased rapidly after infection by WIV2 and 3. In contrast, WIV7-infected mice showed a weaker and delayed response compared with the other two strains. Host antiviral immune response plays an important role in protecting individuals against reovirus infection (Anafu et al., 2013; Dionne et al., 2011; Johansson et al., 2007; Schittone et al., 2012). Reovirus infection induces the production of IFN and proinflammatory cytokines/chemokines (Berard et al., 2012; Schittone et al., 2012). On the one hand, those productions are important for viral clearance, on the other hand, cytokines/chemokines may be associated with tissue damage and diseases (Akdis et al., 2016; Pruijssers et al., 2013; Song et al., 2014). Different reovirus serotypes elicit distinctive pathogenesis and immune response (Douville et al., 2008; Nygaard et al., 2013). The sustained increase of mRNA levels of cytokines/chemokines and peaking later in the infection period may help the virus to progress to systemic infection in the early stage and be responsible for the stronger pathogenicity of WIV7. We also found that WIV7 infection induces a faster neutralisation antibody titre production

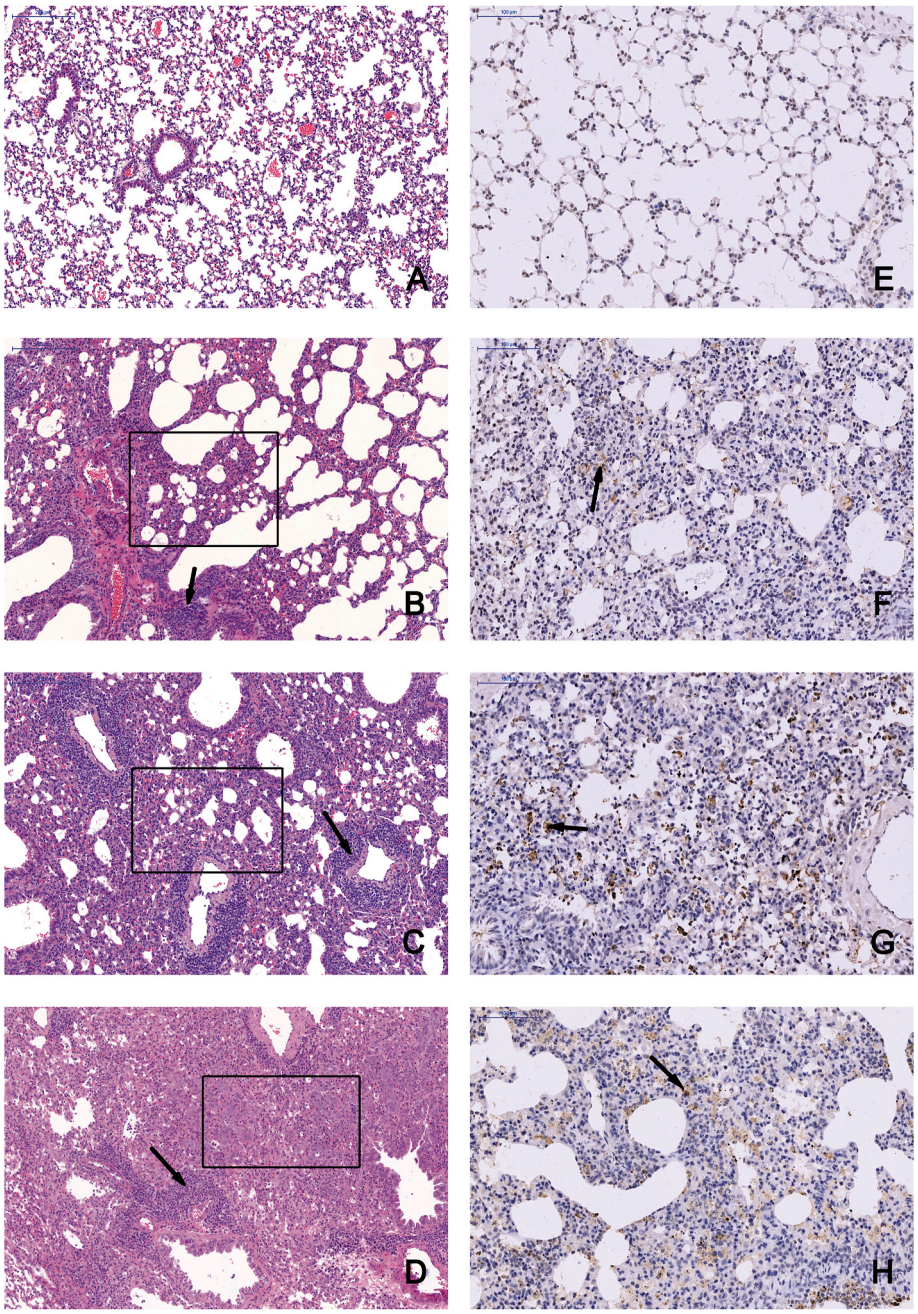

Fig. 4. Bat MRVs infection cause severe pneumonia in BALB/c mice. Left lung lobe of BALB/c mice at 14 dpi were subjected to pathological exam by H&E staining and IHC assay, images were taken from the base of lungs. A and E, mock-infected mice examined by H&E staining and IHC, respectively. B-D, mice infected by WIV2, WIV3 and WIV7, respectively, was examined by H&E staining. The tested tissues showed severe pneumonia with distinct alveolar thickening, reduction of bronchioles and alveoli (black box) and lymphocytic infiltration (black arrow). Scale bar is 200 μm. For IHC assay, rabbit anti-WIV3 polyclonal antibody was used as the primary antibody and HRP-labelled goat anti-rabbit IgG was used as the secondary antibody. The positive area is brownish yellow and can be observed in WIV2- (F), WIV3- (G) and WIV7 (H)-infected lungs. Scale bar is 100 μm.

than WIV2 and WIV3, but since the virus spreads from the primary infected organ to other tissues, neutralising antibodies formed after 7 dpi may not inhibit primary replication (Tyler et al., 1989).

Several studies show that human MRV intranasal infect adult wild type CBA/J mice can cause pneumonia or acute respiratory distress syndrome (Majeski et al., 2003). Intranasal, peroral or intracranially infection can cause systemic dissemination but it's strain-specific dependent (Boehme et al., 2011; Nygaard et al., 2013; Song et al., 2014). Type 1 reoviruses can infect CNS and other tissues through the hematogenous route while type 3 reovirus can use both hematogenous route and neural route access CNS directly (Antar et al., 2009; Boehme et al., 2011; Lai et al., 2015; Morrison et al., 1991). The non-structural σ1s protein was determined to be one of the key molecule of MRV dissemination infection (Boehme et al., 2009; Fleeton et al., 2004). In the tested three bat strains, σ1 and σ1s protein present low amino acid sequence identities compared to each other and meanwhile those proteins show high similarities to some animal and human MRV strains (Supplementary Table S3). Other encoded proteins such as the σ3 protein (encoded by the S4 segment) and the μ2 protein (encoded by the M1 segment) play multiple roles in the control of interferon response (Yue and Shatkin, 1997; Zurney et al., 2009). The residue proline at amino acid (aa) 208 of μ2 protein is critical for repressing interferon signaling pathway (Irvin et al., 2012). We found the aa 208 in the three bat MRV strains were different (WIV2-valine, WIV3-proline, WIV7-proline), which

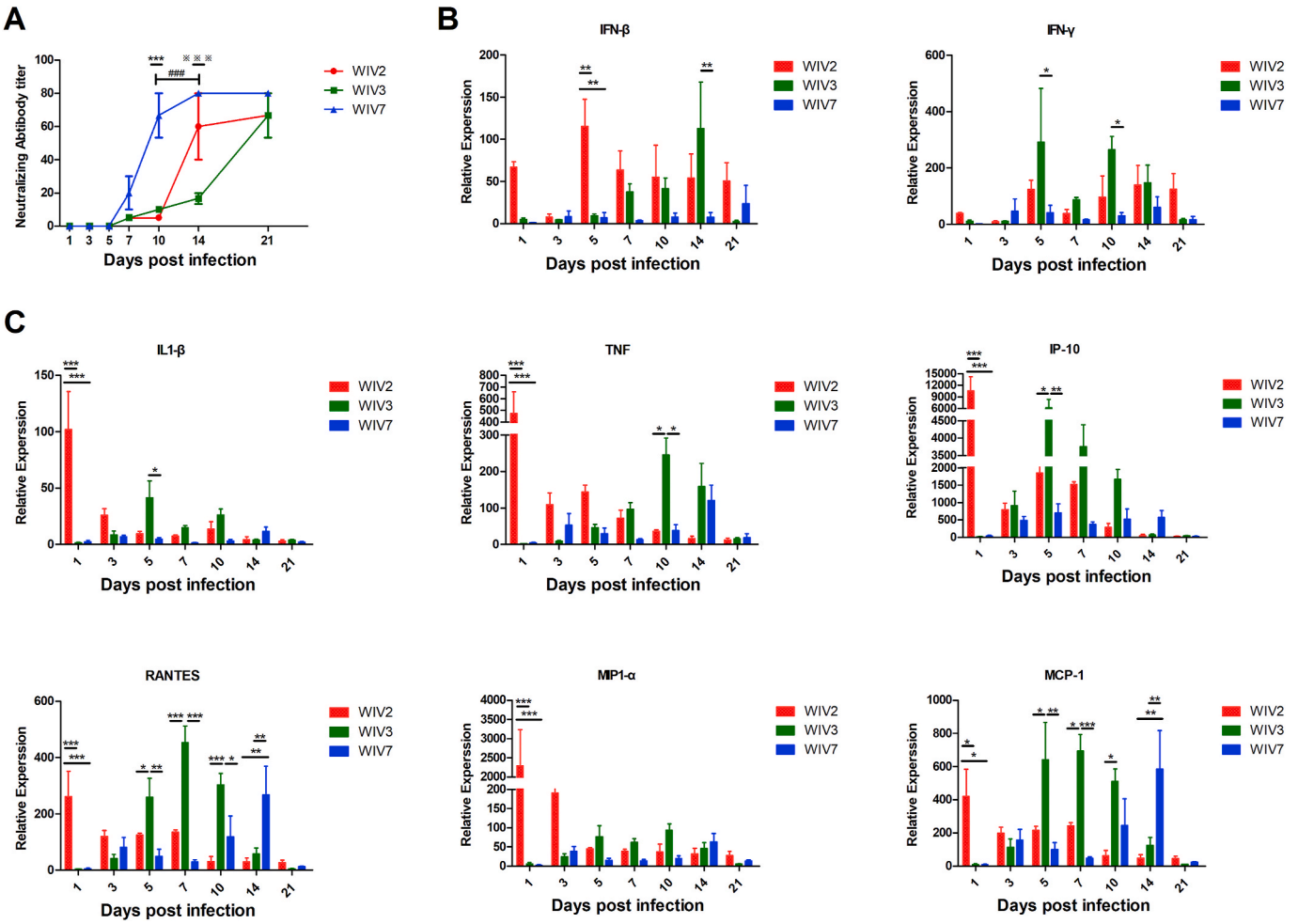

Fig. 5. Bat MRVs induced different patterns of humoral immune response and proinflammatory gene production in BALB/c mice. Infected and mock-infected mice were euthanised at several time points, serum was separated from blood and lungs were collected. Anti-bat MRV neutralisation antibody titres were determined (A). Each serum was measured in triplicate. Titres were expressed as the reciprocal of the final serum dilution required to neutralise all inoculated wells. Total lung RNA was analysed for mRNA expression by RT-qPCR. The gene transcription levels of IFN-β, IFN-γ (B) and proinflammatory cytokines/chemokines (C) were assessed. All data were normalised to 18S rRNA. Relative expression was expressed as the relative fold increase over mock-infected mice. Error bar indicates the standard error. * represent WIV-2 group compared with WIV-7 group, # represent WIV-3 group compared with WIV-7 group, ※ represent WIV-2 group compared with WIV-3 group (A). Black underline represent the comparison between indicated groups (B and C), $*P < 0.05$, $**P < 0.01$, $***P < 0.001$.

may contribute to the high activated immune response of WIV2 and the suppressed response of WIV3 and WIV7 in the early infection stage.

Combing the higher replication in cells and tissues, particularly brain, as well as the more severe damage in lung tissue and weaker and delayed innate immune response in WIV7-infected mice, we suspect that WIV7 has higher pathogenicity than WIV2 and 3, and the WIV2 has the least pathogenicity. Future surveillance should be taken on this virus. In conclusion, we demonstrated the potential risk of bat MRV transmission to humans or other animals by providing evidence of their wide-ranging cell tropism, pathogenicity and immune response in mice. The results showed that some bat MRVs are potentially pathogenic to animal and human populations of which there is no pre-existing antibody due to the MRV transmission route and the close contact between bats and human society. Continuing surveillance of these bat viruses and education to keep away from wild animals should be performed long-term.

Author contribution statement

Ren-Di Jiang: Conceptualization, Methodology, Investigation, Writing-Original Draft Bei Li: Methodology, Resources, Validation Xiang-Ling Liu: Validation Mei-Qin Liu: Investigation Jing Chen: Investigation Dong-Sheng Luo: Validation Bing-Jie Hu: Investigation Wei Zhang: Resources Shi-Yue Li: Resources Xing-Lou Yang: Conceptualization, Methodology, Data Curation, Writing-Review& Editing Zheng-Li Shi: Conceptualization, Formal analysis, Supervision, Writing-Review& Editing.

Acknowledgements

We thank the Center for Instrumental Analysis and Metrology of Wuhan Institute of Virology, CAS, for the assistance in taking confocal microscope pictures (Ding Gao) and histology experiments (Juan Min). We thank the Laboratory Animal Center of Wuhan institute of virology, CAS, for the assistance in animal experiments (Xue-fang An and Fan Zhang).

This study was jointly funded by the National Natural Science Foundation of China Grant (31400143) to XLY. The strategic Priority research Program of the Chinese Academy of Sciences (XDB29010101) to ZLS.

Appendix A. Supplementary data

Supplementary data to this article can be found online at https://doi.org/10.1016/j.virol.2020.05.014.

References

Akdis, M., Aab, A., Altunbulakli, C., Azkur, K., Costa, R.A., Crameri, R., Duan, S., Eiwegger, T., Eljaszewicz, A., Ferstl, R., Frei, R., Garbani, M., Globinska, A., Hess, L., Huitema, C., Kubo, T., Komlosi, Z., Konieczna, P., Kovacs, N., Kucuksezer, U.C., Meyer, N., Morita, H., Olzhausen, J., O'Mahony, L., Pezer, M., Prati, M., Rebane, A., Rhyner, C., Rinaldi, A., Sokolowska, M., Stanic, B., Sugita, K., Treis, A., van de Veen, W., Wanke, K., Wawrzyniak, M., Wawrzyniak, P., Wirz, O.F., Zakzuk, J.S., Akdis, C.A., 2016. Interleukins (from IL-1 to IL-38), interferons, transforming growth factor beta, and TNF-alpha: receptors, functions, and roles in diseases. J. Allergy Clin. Immunol. 138, 984–1010.

Anafu, A.A., Bowen, C.H., Chin, C.R., Brass, A.L., Holm, G.H., 2013. Interferon-inducible transmembrane protein 3 (IFITM3) restricts reovirus cell entry. J. Biol. Chem. 288, 17261–17271.

Antar, A.A., Konopka, J.L., Campbell, J.A., Henry, R.A., Perdigoto, A.L., Carter, B.D., Pozzi, A., Abel, T.W., Dermody, T.S., 2009. Junctional adhesion molecule-A is required for hematogenous dissemination of reovirus. Cell Host Microbe 5, 59–71.

Attoui, H., Biagini, P., Stirling, J., Mertens, P.P., Cantaloube, J.F., Meyer, A., de Micco, P., de Lamballerie, X., 2001. Sequence characterization of Ndelle virus genome segments 1, 5, 7, 8, and 10: evidence for reassignment to the genus Orthoreovirus, family Reoviridae. Biochem. Biophys. Res. Commun. 287, 583–588.

Berard, A.R., Cortens, J.P., Krokhin, O., Wilkins, J.A., Severini, A., Coombs, K.M., 2012. Quantification of the host response proteome after mammalian reovirus T1L infection. PLoS One 7, e51939.

Boehme, K.W., Frierson, J.M., Konopka, J.L., Kobayashi, T., Dermody, T.S., 2011. The reovirus sigma1s protein is a determinant of hematogenous but not neural virus dissemination in mice. J. Virol. 85, 11781–11790.

Boehme, K.W., Guglielmi, K.M., Dermody, T.S., 2009. Reovirus nonstructural protein 1s is required for establishment of viremia and systemic dissemination. Proc. Natl. Acad. Sci. Unit. States Am. 106, 19986–19991.

Botvinkin, A.D., Poleschuk, E.M., Kuzmin, I.V., Borisova, T.I., Gazaryan, S.V., Yager, P., Rupprecht, C.E., 2003. Novel lyssaviruses isolated from bats in Russia. Emerg. Infect. Dis. 9, 1623–1625.

Chua, K.B., Crameri, G., Hyatt, A., Yu, M., Tompang, M.R., Rosli, J., McEachern, J., Crameri, S., Kumarasamy, V., Eaton, B.T., Wang, L.F., 2007. A previously unknown reovirus of bat origin is associated with an acute respiratory disease in humans. Proc. Natl. Acad. Sci. U. S. A. 104, 11424–11429.

Chua, K.B., Koh, C.L., Hooi, P.S., Wee, K.F., Khong, J.H., Chua, B.H., Chan, Y.P., Lim, M.E., Lam, S.K., 2002. Isolation of Nipah virus from Malaysian island flying-foxes. Microb. Infect. 4, 145–151.

Chua, K.B., Voon, K., Crameri, G., Tan, H.S., Rosli, J., McEachern, J.A., Suluraju, S., Yu, M., Wang, L.F., 2008. Identification and characterization of a new orthoreovirus from patients with acute respiratory infections. PLoS One 3, e3803.

Dai, Y., Zhou, Q., Zhang, C., Song, Y., Tian, X., Zhang, X., Xue, C., Xu, S., Bi, Y., Cao, Y., 2012. Complete genome sequence of a porcine orthoreovirus from southern China. J. Virol. 86, 12456.

Day, J.M., 2009. The diversity of the orthoreoviruses: molecular taxonomy and phylogentic divides. Infect. Genet. Evol. 9, 390–400.

Dionne, K.R., Galvin, J.M., Schittone, S.A., Clarke, P., Tyler, K.L., 2011. Type I interferon signaling limits reoviral tropism within the brain and prevents lethal systemic infection. J. Neurovirol. 17, 314–326.

Douville, R.N., Su, R.C., Coombs, K.M., Simons, F.E., Hayglass, K.T., 2008. Reovirus serotypes elicit distinctive patterns of recall immunity in humans. J. Virol. 82, 7515–7523.

Du, L., Lu, Z., Fan, Y., Meng, K., Jiang, Y., Zhu, Y., Wang, S., Gu, W., Zou, X., Tu, C., 2010. Xi River virus, a new bat reovirus isolated in southern China. Arch. Virol. 155, 1295–1299.

Egawa, K., Shimojima, M., Taniguchi, S., Nagata, N., Tani, H., Yoshikawa, T., Kurosu, T., Watanabe, S., Fukushi, S., Saijo, M., 2017. Virulence, pathology, and pathogenesis of Pteropine orthoreovirus (PRV) in BALB/c mice: development of an animal infection model for PRV. PLoS Neglected Trop. Dis. 11, e0006076.

El-Rai, F.M., Evans, A.S., 1963. Reovirus infections in children and young adults. Arch. Environ. Health 7, 700–704.

Fleeton, M.N., Contractor, N., Leon, F., Wetzel, J.D., Dermody, T.S., Kelsall, B.L., 2004. Peyer's patch dendritic cells process viral antigen from apoptotic epithelial cells in the intestine of reovirus-infected mice. J. Exp. Med. 200, 235–245.

Ge, X.Y., Li, J.L., Yang, X.L., Chmura, A.A., Zhu, G., Epstein, J.H., Mazet, J.K., Hu, B., Zhang, W., Peng, C., Zhang, Y.J., Luo, C.M., Tan, B., Wang, N., Zhu, Y., Crameri, G., Zhang, S.Y., Wang, L.F., Daszak, P., Shi, Z.L., 2013. Isolation and characterization of a bat SARS-like coronavirus that uses the ACE2 receptor. Nature 503, 535–538.

Hu, T., Qiu, W., He, B., Zhang, Y., Yu, J., Liang, X., Zhang, W., Chen, G., Zhang, Y., Wang, Y., Zheng, Y., Feng, Z., Hu, Y., Zhou, W., Tu, C., Fan, Q., Zhang, F., 2014. Characterization of a novel orthoreovirus isolated from fruit bat, China. BMC Microbiol. 14, 293.

Irvin, S.C., Zurney, J., Ooms, L.S., Chappell, J.D., Dermody, T.S., Sherry, B., 2012. A single-amino-acid polymorphism in reovirus protein mu2 determines repression of interferon signaling and modulates myocarditis. J. Virol. 86, 2302–2311.

Jansen van Vuren, P., Wiley, M., Palacios, G., Storm, N., McCulloch, S., Markotter, W., Birkhead, M., Kemp, A., Paweska, J.T., 2016. Isolation of a novel fusogenic orthoreovirus from eucampsipoda africana bat flies in South Africa. Viruses 8, 65.

Johansson, C., Wetzel, J.D., He, J., Mikacenic, C., Dermody, T.S., Kelsall, B.L., 2007. Type I interferons produced by hematopoietic cells protect mice against lethal infection by mammalian reovirus. J. Exp. Med. 204, 1349–1358.

Kanai, Y., Kawagishi, T., Okamoto, M., Sakai, Y., Matsuura, Y., Kobayashi, T., 2018. Lethal murine infection model for human respiratory disease-associated Pteropine orthoreovirus. Virology 514, 57–65.

Kohl, C., Lesnik, R., Brinkmann, A., Ebinger, A., Radonic, A., Nitsche, A., Muhldorfer, K., Wibbelt, G., Kurth, A., 2012. Isolation and characterization of three mammalian orthoreoviruses from European bats. PLoS One 7, e43106.

Lai, C.M., Boehme, K.W., Pruijssers, A.J., Parekh, V.V., Van Kaer, L., Parkos, C.A., Dermody, T.S., 2015. Endothelial JAM-A promotes reovirus viremia and bloodstream dissemination. J. Infect. Dis. 211, 383–393.

Leers, W.D., Rozee, K.R., 1966. A survey of reovirus antibodies in sera of urban children. Can. Med. Assoc. J. 94, 1040–1042.

Lelli, D., Moreno, A., Lavazza, A., Bresaola, M., Canelli, E., Boniotti, M.B., Cordioli, P., 2013. Identification of Mammalian orthoreovirus type 3 in Italian bats. Zoonoses Public Health 60, 84–92.

Lelli, D., Moreno, A., Steyer, A., Nagli c, T., Chiapponi, C., Prosperi, A., Faccin, F., Sozzi, E., Lavazza, A., 2015. Detection and characterization of a novel reassortant mammalian orthoreovirus in bats in europe. Viruses 7, 5844–5854.

Leroy, E.M., Kumulungui, B., Pourrut, X., Rouquet, P., Hassanin, A., Yaba, P., Delicat, A., Paweska, J.T., Gonzalez, J.P., Swanepoel, R., 2005. Fruit bats as reservoirs of Ebola virus. Nature 438, 575–576.

Li, Z., Liu, D., Ran, X., Liu, C., Guo, D., Hu, X., Tian, J., Zhang, X., Shao, Y., Liu, S., Qu, L., 2016. Characterization and pathogenicity of a novel mammalian orthoreovirus from wild short-nosed fruit bats. Infect. Genet. Evol. 43, 347–353.

Li, Z., Shao, Y., Liu, C., Liu, D., Guo, D., Qiu, Z., Tian, J., Zhang, X., Liu, S., Qu, L., 2015. Isolation and pathogenicity of the mammalian orthoreovirus MPC/04 from masked civet cats. Infect. Genet. Evol. 36, 55–61.

Lian, H., Liu, Y., Zhang, S., Zhang, F., Hu, R., 2013. Novel orthoreovirus from mink, China, 2011. Emerg. Infect. Dis. 19, 1985–1988.

Lorusso, A., Teodori, L., Leone, A., Marcacci, M., Mangone, I., Orsini, M., Capobianco-Dondona, A., Camma, C., Monaco, F., Savini, G., 2015. A new member of the Pteropine Orthoreovirus species isolated from fruit bats imported to Italy. Infect. Genet. Evol. 30, 55–58.

Majeski, E.I., Harley, R.A., Bellum, S.C., London, S.D., London, L., 2003. Differential role for T cells in the development of fibrotic lesions associated with reovirus 1/L-induced bronchiolitis obliterans organizing pneumonia versus Acute Respiratory Distress Syndrome. Am. J. Respir. Cell Mol. Biol. 28, 208–217.

Matsuura, K., Ishikura, M., Nakayama, T., Hasegawa, S., Morita, O., Katori, K., Uetake, H., 1993. Ecological studies on reovirus pollution of rivers in Toyama Prefecture. II. Molecular epidemiological study of reoviruses isolated from river water. Microbiol. Immunol. 37, 305–310.

Matsuura, K., Ishikura, M., Nakayama, T., Hasegawa, S., Morita, O., Uetake, H., 1988. Ecological studies on reovirus pollution of rivers in Toyama Prefecture. Microbiol. Immunol. 32, 1221–1234.

Mayor, H.D., Jamison, R.M., Jordan, L.E., Vanmitchell, M., 1965. Reoviruses. Ii. Structure and composition of the virion. J. Bacteriol. 89, 1548–1556.

Morrison, L.A., Sidman, R.L., Fields, B.N., 1991. Direct spread of reovirus from the intestinal lumen to the central nervous system through vagal autonomic nerve fibers. Proc. Natl. Acad. Sci. U. S. A. 88, 3852–3856.

Nygaard, R.M., Lahti, L., Boehme, K.W., Ikizler, M., Doyle, J.D., Dermody, T.S., Schiff, L.A., 2013. Genetic determinants of reovirus pathogenesis in a murine model of respiratory infection. J. Virol. 87, 9279–9289.

Ouattara, L.A., Barin, F., Barthez, M.A., Bonnaud, B., Roingeard, P., Goudeau, A., Castelnau, P., Vernet, G., Paranhos-Baccala, G., Komurian-Pradel, F., 2011. Novel human reovirus isolated from children with acute necrotizing encephalopathy. Emerg. Infect. Dis. 17, 1436–1444.

Pritchard, L.I., Chua, K.B., Cummins, D., Hyatt, A., Crameri, G., Eaton, B.T., Wang, L.F., 2006. Pulau virus; a new member of the Nelson Bay orthoreovirus species isolated from fruit bats in Malaysia. Arch. Virol. 151, 229–239.

Pruijssers, A.J., Hengel, H., Abel, T.W., Dermody, T.S., 2013. Apoptosis induction influences reovirus replication and virulence in newborn mice. J. Virol. 87, 12980–12989.

Rosen, L., 1960. Serologic grouping of reoviruses by hemagglutination-inhibition. Am. J. Hyg. 71, 242–249.

Sabin, A.B., 1959. Reoviruses. A new group of respiratory and enteric viruses formerly classified as ECHO type 10 is described. Science 130, 1387–1389.

Schittone, S.A., Dionne, K.R., Tyler, K.L., Clarke, P., 2012. Activation of innate immune responses in the central nervous system during reovirus myelitis. J. Virol. 86, 8107–8118.

Song, L., Lu, Y., He, J., Yu, Y., Zuo, T., Li, Y., Zhu, H., Duan, Q., 2014. Multi-organ lesions in suckling mice infected with SARS-associated mammalian reovirus linked with apoptosis induced by viral proteins mu1 and sigma1. PLoS One 9, e92678.

Steyer, A., Gutierrez-Aguire, I., Kolenc, M., Koren, S., Kutnjak, D., Pokorn, M., Poljsak-Prijatelj, M., Racki, N., Ravnikar, M., Sagadin, M., Fratnik Steyer, A., Toplak, N., 2013. High similarity of novel orthoreovirus detected in a child hospitalized with acute gastroenteritis to mammalian orthoreoviruses found in bats in Europe. J. Clin. Microbiol. 51, 3818–3825.

Teeling, E.C., Springer, M.S., Madsen, O., Bates, P., O'Brien S, J., Murphy, W.J., 2005. A molecular phylogeny for bats illuminates biogeography and the fossil record. Science 307, 580–584.

Tyler, K.L., Barton, E.S., Ibach, M.L., Robinson, C., Campbell, J.A., O'Donnell, S.M., Valyi-Nagy, T., Clarke, P., Wetzel, J.D., Dermody, T.S., 2004. Isolation and molecular characterization of a novel type 3 reovirus from a child with meningitis. J. Infect. Dis. 189, 1664–1675.

Tyler, K.L., Virgin, H.W.t., Bassel-Duby, R., Fields, B.N., 1989. Antibody inhibits defined stages in the pathogenesis of reovirus serotype 3 infection of the central nervous system. J. Exp. Med. 170, 887–900.

Vasquez, C., Tournier, P., 1962. The morphology of reovirus. Virology 17, 503–510.

Voon, K., Chua, K.B., Yu, M., Crameri, G., Barr, J.A., Malik, Y., Wang, L.F., 2011. Evolutionary relationship of the L- and M-class genome segments of bat-borne

fusogenic orthoreoviruses in Malaysia and Australia. J. Gen. Virol. 92, 2930–2936.
Waruhiu, C., Ommeh, S., Obanda, V., Agwanda, B., Gakuya, F., Ge, X.Y., Yang, X.L., Wu, L.J., Zohaib, A., Hu, B., Shi, Z.L., 2017. Molecular detection of viruses in Kenyan bats and discovery of novel astroviruses, caliciviruses and rotaviruses. Virol. Sin. 32, 101–114.
Yang, X.L., Hu, B., Wang, B., Wang, M.N., Zhang, Q., Zhang, W., Wu, L.J., Ge, X.Y., Zhang, Y.Z., Daszak, P., Wang, L.F., Shi, Z.L., 2015a. Isolation and characterization of a novel bat coronavirus closely related to the direct progenitor of severe acute respiratory syndrome coronavirus. J. Virol. 90, 3253–3256.
Yang, X.L., Tan, B., Wang, B., Li, W., Wang, N., Luo, C.M., Wang, M.N., Zhang, W., Li, B., Peng, C., Ge, X.Y., Zhang, L.B., Shi, Z.L., 2015b. Isolation and identification of bat viruses closely related to human, porcine and mink orthoreoviruses. J. Gen. Virol. 96, 3525–3531.
Yue, Z., Shatkin, A.J., 1997. Double-stranded RNA-dependent protein kinase (PKR) is regulated by reovirus structural proteins. Virology 234, 364–371.
Zeng, L.P., Gao, Y.T., Ge, X.Y., Zhang, Q., Peng, C., Yang, X.L., Tan, B., Chen, J., Chmura, A.A., Daszak, P., Shi, Z.L., 2016. Bat severe acute respiratory syndrome-like coronavirus WIV1 encodes an extra accessory protein, ORFX, involved in modulation of the host immune response. J. Virol. 90, 6573–6582.
Zurney, J., Kobayashi, T., Holm, G.H., Dermody, T.S., Sherry, B., 2009. Reovirus mu2 protein inhibits interferon signaling through a novel mechanism involving nuclear accumulation of interferon regulatory factor 9. J. Virol. 83, 2178–2187.